Fabrication of a highly efficient core-mode blocker using a femtosecond laser ablation technique

Sun Do Lim[1,3*], Jae Gu Kim[2], Kwanil Lee[3], Sang Bae Lee[3], and Byoung Yoon Kim[1]

[1]*Department of Physics, Korea Advanced Institute of Science and Technology (KAIST), Daejeon, 305-701, Korea*
[2] *Nano-Mechanical Systems Research Division, Korea Institute of Machinery & Materials (KIMM), Daejeon, 305-343, Korea*
[3]*Photonics Research Laboratory, Korea Institute of Science and Technology (KIST), Seoul, 136-791, Korea*
** sdlim@kist.re.kr*

Abstract: We present a method for the fabrication of a highly efficient core-mode blocker based on a laser micromachining technique. The process for the fabrication is as follows. A micron-sized crater is made by irradiation of an ultra-short pulse laser on the end face of a single-mode fiber, and then a defect that acts as a core-mode blocker is formed by splicing the cratered fiber with a normal fiber. The attenuation of the core mode was adjustable up to 25dB according to the initial crater size and the splicing condition. An all-fiber acousto-optic tunable bandpass filter built with the core-mode blocker is also demonstrated, which exhibits a low insertion loss of 1.8dB with non-resonance light suppression greater than 23dB.

OCIS codes: (060.2310) Fiber optics; (140.3440) Laser-induced breakdown; (230.1040) Acousto-optical devices.

References and links

1. S. H. Yun, I. K. Hwang, and B. Y. Kim, "All-fiber tunable filter and laser based on two mode fiber," Opt. Lett. **21**(1), 27–29 (1996).
2. H. S. Kim, S. H. Yun, I. K. Hwang, and B. Y. Kim, "All-fiber acousto-optic tunable notch filter with electronically controllable spectral profile," Opt. Lett. **22**(19), 1476–1478 (1997).
3. I. K. Hwang, S. H. Yun, B. Y. Kim, "All-fiber tunable comb filter with nonreciprocal transmission," IEEE Photon. Technol. Lett. **10**(10), 1437–1439 (1998).
4. M. S. Lee, I. K. Hwang, and B. Y. Kim, "Acousto-optic tunable bandpass filter," in Proc. OECC/IOOC 2001, pp. 324–325 (2001).
5. K. J. Lee, D. I. Yeom, and B. Y. Kim, "Narrowband, polarization insensitive all-fiber acousto-optic tunable bandpass filter," Opt. Express **15**(6), 2987–2992 (2007).
6. D. S. Starodubov, V. Grubsky, and J. Feinberg, "All-fiber Bandpass Filter with Adjustable Transmission Using Cladding-Mode Coupling," IEEE Photon. Technol. Lett. **10**(11), 1590–1592 (1998).
7. Y. G. Han, S. H. Kim, S. B. Lee, U. C. Paek, and Y. Chung, "Development of core mode blocker with H2-loaded Ge-B codoped fibres," Electron. Lett. **39**(15), 1107–1108 (2003).
8. M. Lenzner, J. Krüger, S. Sartania, Z. Cheng, Ch. Spielmann, G. Mourou, W. Kautek, and F. Krausz, "Femtosecond Optical Breakdown in Dielectrics," Phys. Rev. Lett. **80**(18), 4076–4079 (1998).
9. R. Stoian, D. Ashkenasi, A. Rosenfeld, and E. E. B. Campbell, "Coulomb explosion in ultra-short pulsed laser ablation of Al2O3," Phys. Rev. B **62**(19), 13167–13173 (2000).

1. Introduction

A bandpass filter is one of the key components for flexible wavelength manipulation in wavelength-division-multiplexed (WDM) optical network, optical sensor, and spectrum analyzing and tunable laser systems. Particularly, an all-fiber acousto-optic tunable bandpass filter (AOTBF) has attracted much attention due to the outstanding performances such as low insertion loss, broad tuning range, and fast tuning speed [1–3]. The simplest configuration of the all-fiber AOTBF consists of an acoustic long period grating (LPG) and a core-mode blocker located at the mid-point of the grating length [4,5]. The first part of the acoustic grating couples the core-mode light to anti-symmetric cladding modes at resonance wavelengths, and the second part of the grating couples the cladding-mode light back into the

#114644 - $15.00 USD Received 22 Jul 2009; revised 2 Sep 2009; accepted 20 Sep 2009; published 28 Sep 2009

core. The core-mode blocker located in the middle of the interaction length attenuates the non-resonance core-mode light transmission, resulting in a bandpass filtering in the transmission spectrum at the resonance wavelength. The ideal core-mode blocker requires a large attenuation for the core mode and low loss transmission for the cladding modes. To date, there have been various attempts to fabricate the core-mode blocker by using HF etching [5], intense UV laser including KrF laser [4,6], and electric arc discharge [7]. The HF etching method uses the etching speed difference between Ge-doped core and pure-silica cladding in the fiber. However, owing to small difference between the etch rates for core and cladding, it is difficult to control the parameters involved in the fabrication. Moreover, the etched outer cladding perturbs the optical and the acoustic propagation, thereby severely deteriorating the device performance. The method using the KrF lasers introduces a damage track between core and cladding boundary of dispersion compensating fiber (DCF) wherein hydrogen is loaded into a highly Ge-doped core for up to a week before the laser exposure. The electric arc discharge method produces an air bubble in the core after local heating treatment on the hydrogen loaded GeB co-doped fiber. These two methods are very restrictive in the fiber selection and time-consuming due to the pretreatment of hydrogen loading. In addition, the length of the core-mode blocker reaches up to a few centimeters, which increases the insertion loss of the devices.

In this paper, we propose and demonstrate a novel method for fabrication of a highly efficient core-mode blocker by using a femtosecond laser ablation technique on a conventional SMF. The method produces a micron-sized mechanical damage at the core of the cleaved end face of the fiber leading to a defect (bubble) after splicing process. The defect efficiently suppresses only the core-mode power resulting in a core-mode blocker. We also demonstrate an all-fiber acousto-optic tunable bandpass filter (AOTBF) composed of the fabricated core-mode blocker, and characterize the device performance.

2. Fabrication of the core-mode blocker

We used an ultra-short pulse laser ablation technique for the fabrication of a core-mode blocker. The output of the Ti:sapphire laser system used for the experiment had 220-fs pulse width, 100-kHz repetition rate, and 450-mW average power at the 800-nm operation wavelength. The average power of the laser beam at the sample location was 100 mW. Beam waist at the focal point and depth of focus are about 2.44 μm (calculated based on the diffraction optics) and 3.74 μm (calculated based on the energy density criterion), respectively. The laser beam was tightly focused by a microscope objective on the center of a cleaved SMF (Samsung, core/cladding diameter: 9.3/125 μm). Figure 1(a) shows the configuration of the experimental setup for making the crater in the core of the fiber.

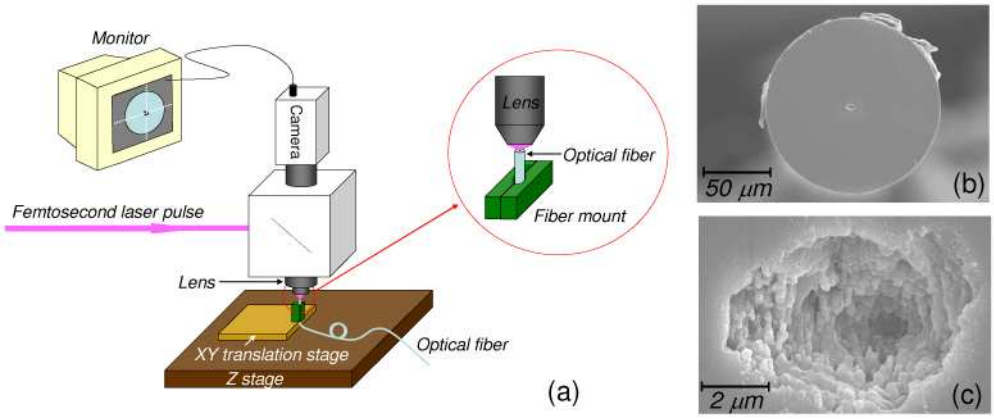

Fig. 1. (a) Experimental setup for the fabrication of the crater in the core of the fiber (b) Cleaved end face of the fiber with the crater and (c) enlarged view of the crater

#114644 - $15.00 USD Received 22 Jul 2009; revised 2 Sep 2009; accepted 20 Sep 2009; published 28 Sep 2009

When the fiber was irradiated by the laser pulse for 2 seconds, a micron-sized crater was generated at the focal point as shown in Fig. 1(b) and (c). The machined crater was examined using a scanning electron microscopy (SEM). In this case, we used an objective lens with NA of 0.4, which leads the diameter and the depth of the crater to be about 7 and 6 μm, respectively for the given laser pulse power. It should be noted that we used three different types of objective lenses in order to find out the relation between crater size and NA value. For the lenses with NA values of 0.4 and 0.8, the mean diameter of the crater was about 6 and 2 μm, respectively. For the other lens with NA of 0.25, the crater diameter was over 15 μm. In our experiment, the objective lens with NA of 0.4 was chosen because the formed crater with the size of 6~7 micron can be transformed to the intended size of a defect during splicing process in next step. It is worth noting that the crater-forming mechanism can be interpreted as impulsive, macroscopic Coulomb explosion (CE) of the charged dielectric surface [8,9]. Thus, the dominant mechanism for creating the crater is to mechanically break the dielectric, so-called 'cold ablation', not to melt by the thermal effect.

We made a defect in the core by splicing the crater-formed fiber with the same fiber having a normal cleaved end as shown in Fig. 2(a) and (b).

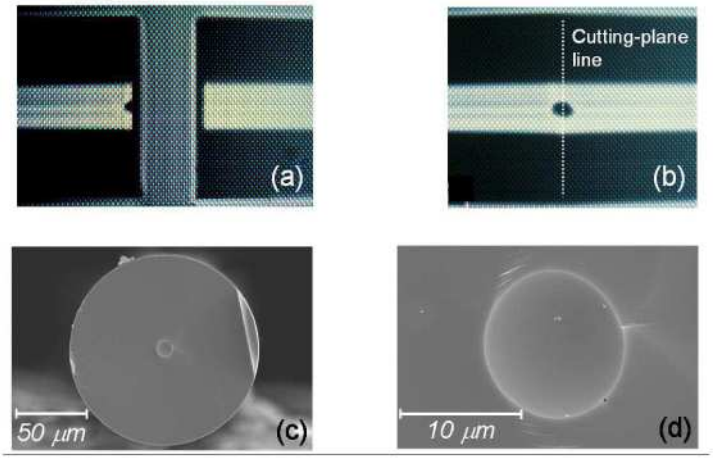

Fig. 2. Splicer panel views (a) before and (b) after the fibers are spliced. The splice was carried out by using an arc fusion splicer (FSM-30S, Fujikura) (c) Cross-section view of the bubble and (d) enlarged view of it.

The splicing conditions such as arc power and arc time are very important because they define the final size of the defect that determines the insertion loss of the device. Particularly, the short arc time is preferred. In our case, the arc power level and time were 35 and 0.4 s, respectively. The experimental results show that the crater can be formed into a defect with a good reproducibility (almost 100%) under the given splicing conditions. Figure 2(c) and (d) shows the cross section of the spheroidal-shaped defect which was generated from the crater. The size of the defect was measured to be about 11.6 μm in equatorial diameter and 10 μm in polar diameter (longitudinal axis). It was experimentally found that a longer arc-time or an additional arc exposure results in the degradation of the core-mode suppression despite the defect growth of up to 50%. Figure 3 compares two examples of the transmission spectra for core-mode blockers formed by different arc conditions; 2-second arc exposure for the upper defect and 0.4-second for lower one. As one can see, the core-mode blocker with a 20-μm diameter induces only about 5dB transmission loss whereas that with an 11-μm diameter introduces 25dB loss. We believe that the additional arc exposure tends to make the defect to be more evenly rounded.

#114644 - $15.00 USD Received 22 Jul 2009; revised 2 Sep 2009; accepted 20 Sep 2009; published 28 Sep 2009

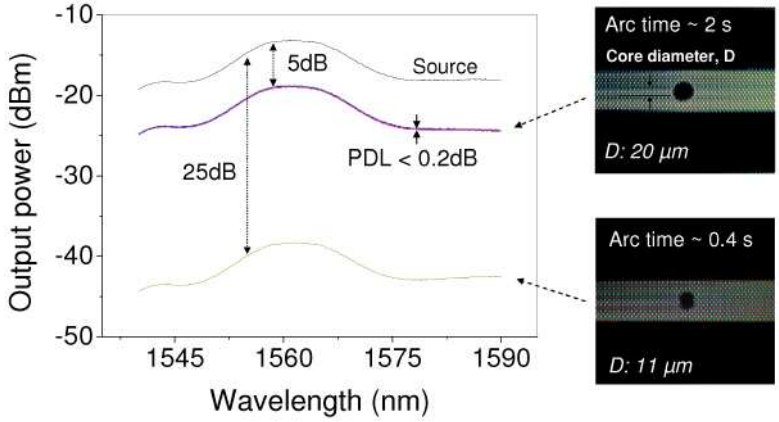

Fig. 3. Transmission spectra of the two different sized core-mode blockers

Figure 4 shows the calculated losses of LP_{01} core and LP_{11} cladding mode as a function of the size of the defect and the experimental results.

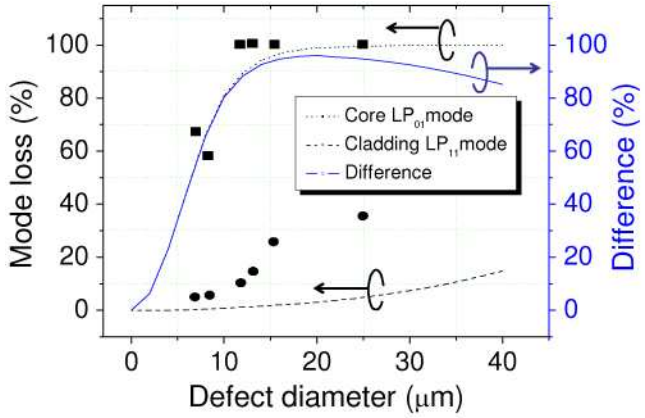

Fig. 4. Calculation of transmission loss by the defect as a function of the defect diameter for the core LP_{01} and the cladding LP_{11} modes at 1.55 μm. Experimental results are also plotted (Solid square for the core mode and solid circle for the cladding mode)

The calculation was carried out under the assumption that the loss is determined entirely by the ratio of the optical signal power in the area occupied by the defect to the total power in the mode. The effect of the axial length of the defect on the loss was not considered in the calculation. According to the calculation results, the maximum loss difference between the core and the cladding modes occurs at the defect diameter ranging from 16 to 22 μm. It is attributed to the fact that the major power of the core mode is confined in the core region whereas that of the cladding mode is in the cladding region. In real situation, other physical parameters such as axial length, the surface state and the shape of the defect also influence on the loss difference. Experimental finding showed that the core-mode loss is proportional to the size of the defect when it is smaller than the core diameter. However, when the defect is bigger than the core diameter, its surface roughness becomes a dominant factor that determines the core-mode loss. In comparison, the loss of the cladding LP_{11} mode increased continuously as the defect diameter increased. Therefore, the maximum extinction could be achieved when the defect had a diameter similar to that of the core and rough surface condition. We could experimentally find proper arc power and time duration under which the craters are expanded into 10~12-μm-sized defects with rough surface during the splicing process for optimum performances. Figure 5 shows the loss spectrum of the core mode blocker with a diameter of 12.1 μm and a length of 9.7 μm as a function of the wavelength.

#114644 - $15.00 USD Received 22 Jul 2009; revised 2 Sep 2009; accepted 20 Sep 2009; published 28 Sep 2009

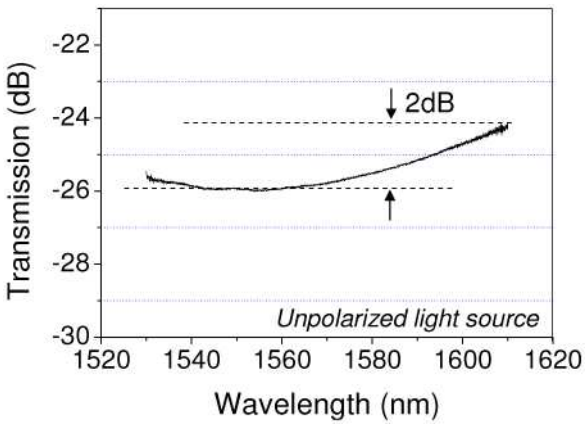

Fig. 5. Core-mode loss spectrum of the core-mode blocker for an unpolarized light source

It shows that the core-mode attenuation is larger than 24dB over the wavelength range of our interest, and the polarization dependent loss is negligible. It was empirically found that about 42% of the scattered light is coupled to forward propagating higher order cladding modes. The rest of the scattered light is considered to be either coupled to backward propagating cladding modes or radiated. It is worth noting that the defect has an uneven surface along with an arbitrary shape (typically non-circular), which gives rise to a diffuse reflection. To this end, it was difficult to observe the etalon effect taking place between inside surfaces of the defect. The back reflected core-mode light was also measured to be less than 1%. For the band-pass filter application, the unwanted cladding modes excited by the defect at non-resonance wavelength do not couple back into the core and are removed by the fiber jacket at the end of the interaction region. The loss of the cladding LP_{11} mode coupled at resonance wavelength will be discussed in the last part of the paper.

3. All-fiber acousto-optic bandpass filter

We constructed a SMF AOTBF using the fabricated core-mode blocker. The basic configuration and the working principle of the device is similar to that described in Ref [2,4]. The acousto-optic interaction length of the device was 32 cm. The AOTBF utilizes mode coupling between the core and the cladding modes produced by the traveling acoustic flexural wave. The core-mode blocker was located at the mid-point of the acousto-optic interaction length of the device. As mentioned in previous section, the first part of the interaction length couples the light from the core mode to the phase-matched cladding modes. The core-mode blocker attenuates the propagating core-mode light, but the coupled (i.e., phase-matched) cladding modes at resonance wavelengths propagates without a significant loss. The second part couples the light in the cladding modes back into the core. Thus, the device can pass the light at the resonance wavelengths and suppress the non-resonance light transmission. The mode coupling involved in the filter was between the LP_{01} core and the LP_{11} cladding modes. Figure 6(a) shows the transmission spectrum of the device at the applied frequency of 1.98 MHz. The filter shows the insertion loss of about 1.8dB and a 3-dB bandwidth of 1.42 nm that compares well with the calculated value of 1.53 nm. Non-resonance wavelength suppression ratio was found to be ~23 dB. Polarization dependent center-wavelength splitting was also measured to be about 0.26 nm. The resonance wavelength is plotted as a function of the applied acoustic frequency in Fig. 6(b). The tuning slope of the resonance wavelength was almost linear over the wavelength range of 100 nm. Here, the total insertion loss of the device was closely related to the cladding LP_{11} mode loss by the defect and the incomplete over-coupling.

#114644 - $15.00 USD Received 22 Jul 2009; revised 2 Sep 2009; accepted 20 Sep 2009; published 28 Sep 2009

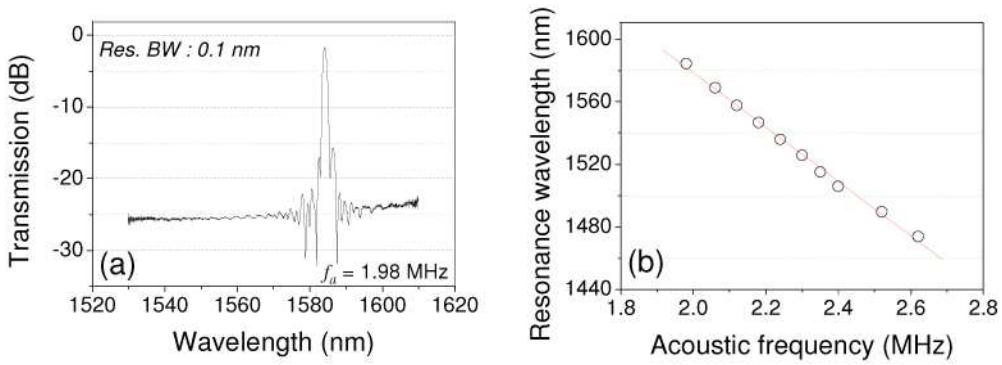

Fig. 6. (a) Transmission spectrum of the AOTBF (b) Resonance wavelength as a function of the applied acoustic frequency

The incompleteness of the overcoupling is originated from the different propagation constants of constituent true modes of the cladding LP_{11} mode that results in the change in the intensity lobe orientation. The loss arising from the overcoupling process was estimated to be about 1.36dB from the transmission spectrum that is shown in Fig. 7.

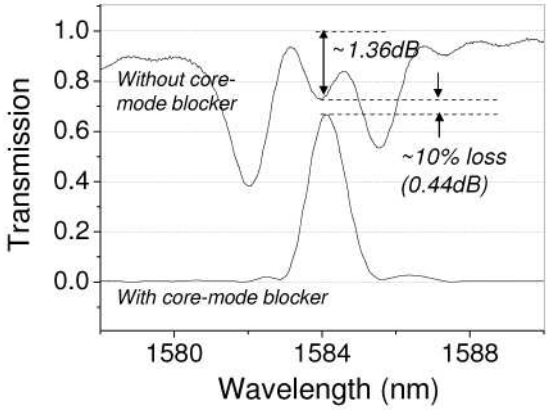

Fig. 7. Comparison of the transmission spectra of the AOTFs with the air bubble and without the air bubble (Interaction length: 32 cm, Applied acoustic frequency: 1.98 MHz)

The figure also compares the over-coupling transmission spectrum (in the case of no core-mode blocker) to the transmission spectrum in the presence of the core-mode blocker under the linear scale. The 10% loss (0.44dB) shown in the figure is presumably considered to be the cladding LP_{11} mode loss by the defect (core-mode blocker).

4. Conclusion

We proposed a novel method for the fabrication of a highly efficient core-mode blocker by using a femtosecond laser ablation technique. The crater with an about 7-μm diameter was laser-ablated using a lens of NA 0.4, which results in an about 11-μm sized defect (bubble) in the core acting as an efficient core-mode blocker after splicing under the proper conditions. The suppression of the core mode by the core-mode blocker was 25dB while the attenuation of the cladding mode was deducted to be 0.44dB. An all-fiber AOTBF with the core-mode blocker was also demonstrated, which shows a low insertion loss of 1.8dB and a high suppression of non-resonance light more than 23dB.

Acknowledgements

This work was partially supported by the Korea Research Foundation Grant funded by the Korean Government (KRF-2008-313-C00350).

#114644 - $15.00 USD Received 22 Jul 2009; revised 2 Sep 2009; accepted 20 Sep 2009; published 28 Sep 2009